

## Supplementary Information

### Growth of {100}-oriented lead zirconate titanate thin films mediated by a safe solvent

Nicolas Godard,<sup>\*a</sup> Emmanuel Defay,<sup>\*a</sup> Patrick Grysan,<sup>a</sup> and Sebastjan Glinšek<sup>a</sup>

<sup>a</sup> Materials Research and Technology (MRT) department,  
Luxembourg Institute of Science and Technology (LIST)

\* Corresponding authors: [nicolasgodard@live.be](mailto:nicolasgodard@live.be), [emmanuel.defay@list.lu](mailto:emmanuel.defay@list.lu)

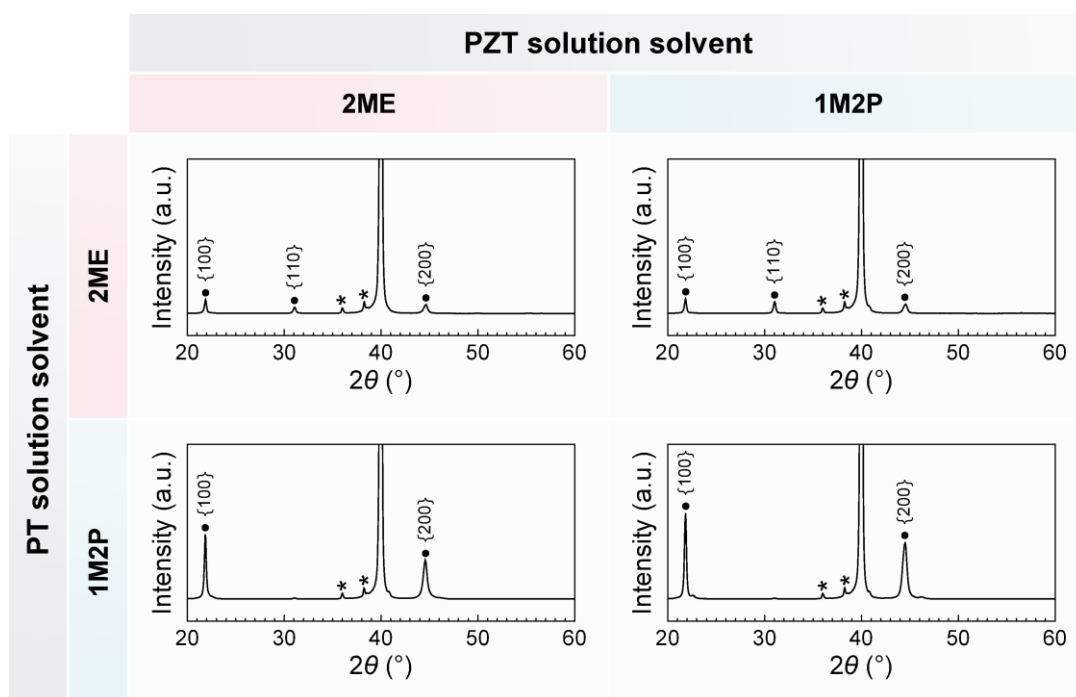


**Figure S1** – Cross check experiment: XRD patterns of 200 nm-thick PZT films as function of the solvents used for the PbTiO<sub>3</sub> (PT) seed layer and the PZT film. The peaks marked with asterisks (\*) are due to the substrate. The scale is identical for all the XRD patterns.

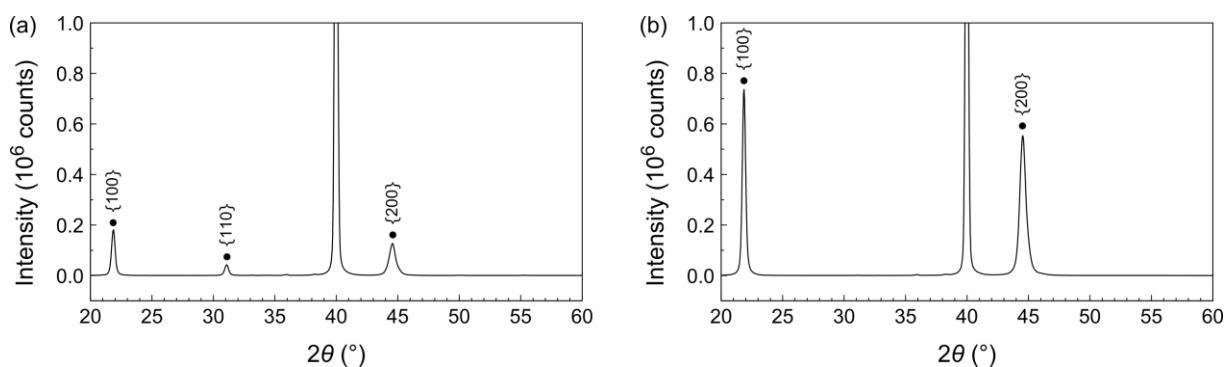


**Figure S2** – XRD patterns of micron-thick PZT thin films deposited on platinumized silicon using (a) 2ME and (b) 1M2P-based solutions (PbTiO<sub>3</sub> seed layer and PZT film). Note that the absolute scale is identical for both XRD patterns (linear scale).

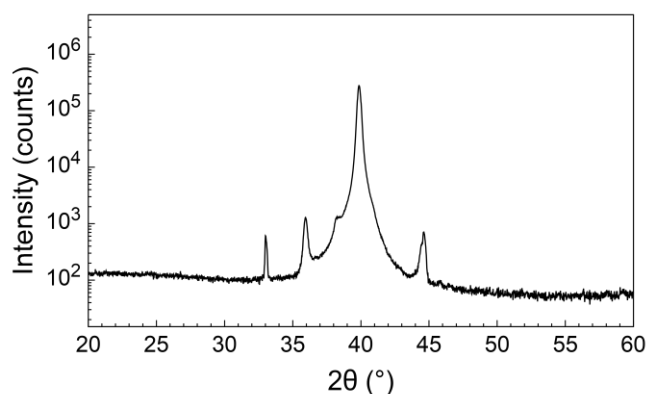


**Figure S3** – X-ray diffraction pattern of a bare platinumized silicon substrate showing the parasitic peaks that appear in the patterns of Figs. 2 and 3. Platinum is always characterized by two signals: the main Pt(111) reflection at  $2\theta \sim 40^\circ$  and the one due to the fact that the X-ray beam is not perfectly monochromatic. The Pt(111) reflection at  $36^\circ$  is due to copper  $K_\beta$  ( $\lambda = 1.39225 \text{ \AA}$ ) radiation. The signal at  $33^\circ$  can be attributed to the Si(200) forbidden reflection. The shoulder at  $38^\circ$  and the peak at  $44.5^\circ$  could not be identified precisely, but they can be both considered as substrate contributions.

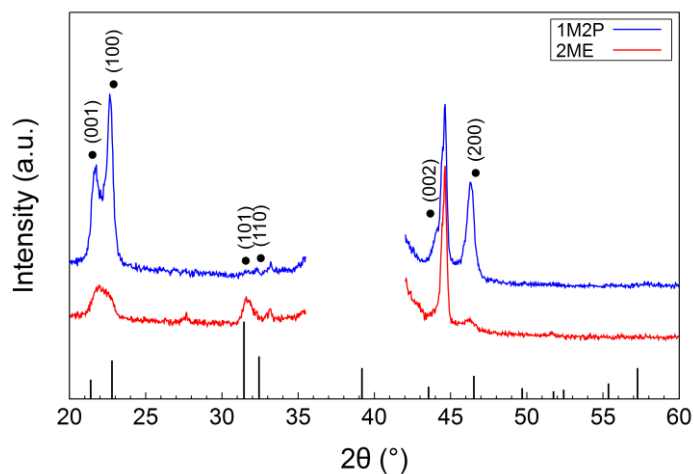


**Figure S4** – XRD patterns of PbTiO<sub>3</sub> seed layers deposited using 2ME and 1M2P-based solutions (linear scale).

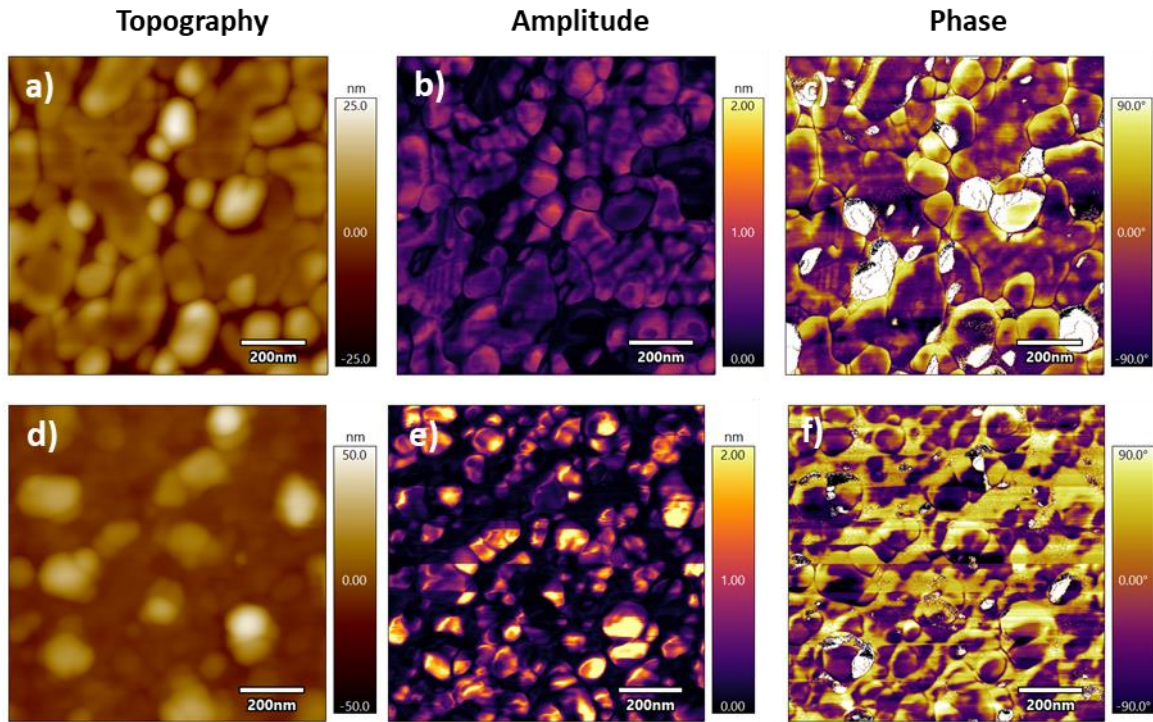


**Figure S5** – Topography (a, d), out-of-plane PFM amplitude (b, e) and phase (c, f) of  $\text{PbTiO}_3$  seed layers prepared from 2ME-based (a, b, c) and 1M2P-based (d, e, f) solutions.

In order to obtain an increased sensitivity, the piezoforce microscopy (PFM) measurements of the  $\text{PbTiO}_3$  seed layers films have been conducted on an MFP3D Infinity AFM (Asylum Research, Santa Barbara) at the contact resonance with a Dual Amplitude Resonance Tracking monitoring of the contact resonance frequency shifts. A 4 kHz and a 2 V amplitude sine wave bias was injected on the conductive tip, creating two side bands around the contact resonance. The Lock-In demodulation of the lowest frequency side band was used to image the PFM amplitude and phase responses.

The AFM tip used was a conductive Pt/Ir coated Asyelec (Asylum Research, Santa Barbara) with a typical cantilever stiffness of 2 N/m and resonance of 70 kHz. The contact resonance is found around 320 kHz. The back electrode of the samples was connected to the ground of the instrument and the electrical path was checked for a few ohms resistance with a multimeter. Switching spectroscopy PFM (SS-PFM) curves were measured again by demodulating the lower frequency side band after 10 ms DC bias pulses following a triangular sawtooth pattern ranging from  $-7$  V to 7 V.

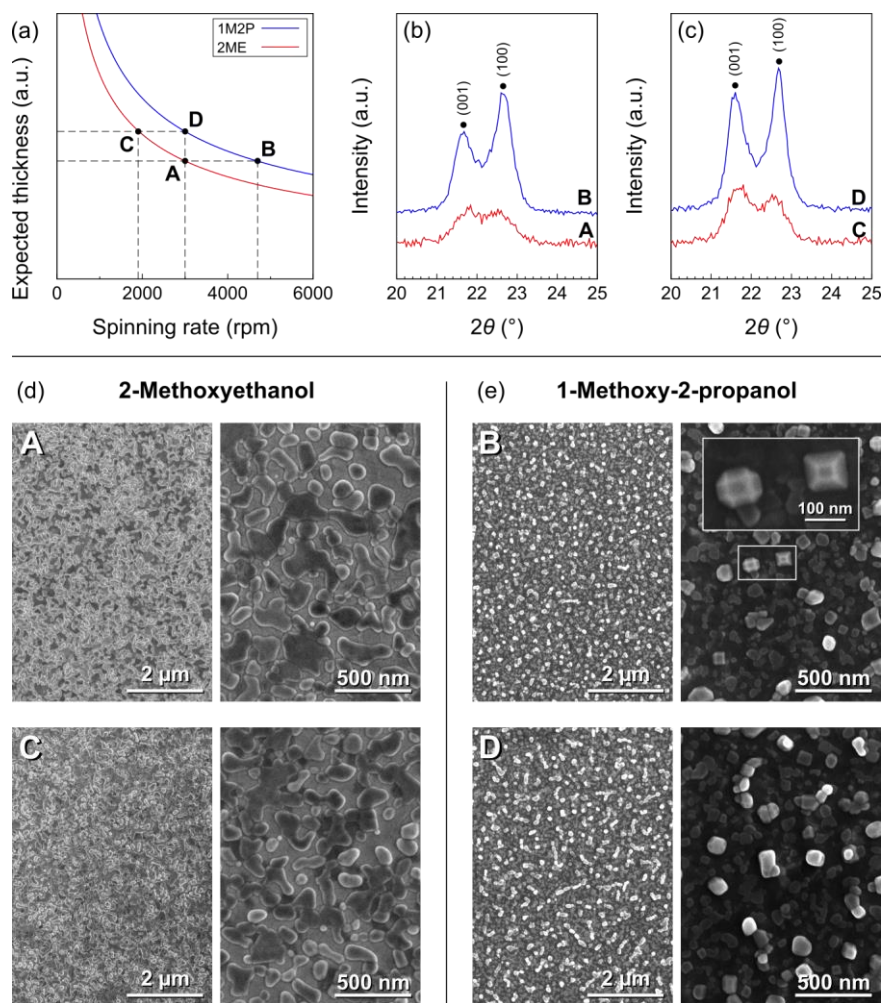


**Figure S6** – Influence of the spinning rate on the microstructure of  $\text{PbTiO}_3$  seed layers. (a) Evolution of the thickness of the liquid deposited film based on the  $\propto \frac{1}{\sqrt{\omega}}$  model. (b) and (c) show the XRD patterns of the (100)/(001) reflection and surface SEM micrographs are shown in (d) and (e) for 2ME and 1M2P-derived seed layers, respectively.

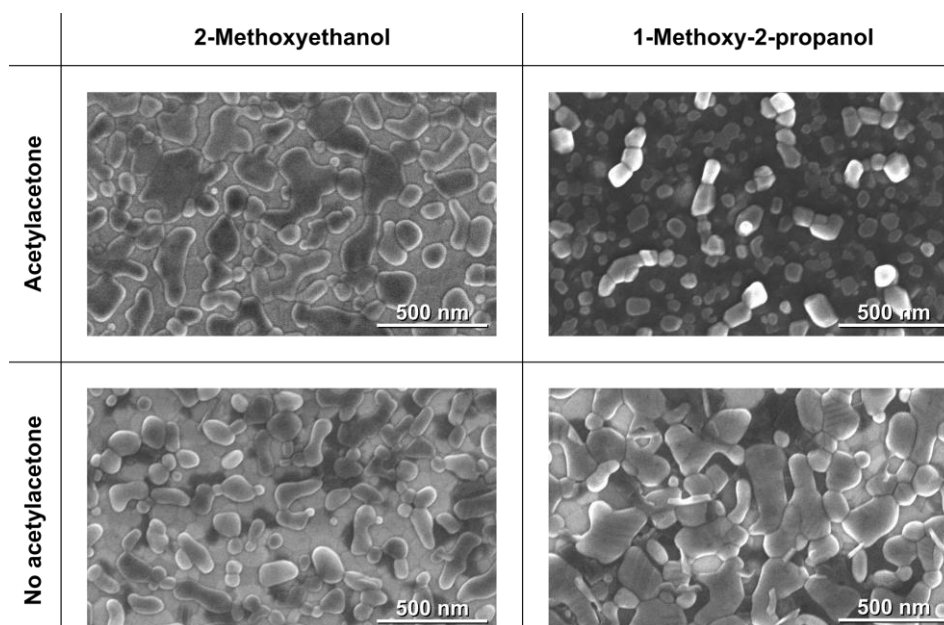


**Figure S7** – SEM top views showing the influence of the presence of acetylacetonone on the microstructure of  $\text{PbTiO}_3$  seed layers derived from 2ME and 1M2P-based solutions. For all the samples, the spinning rate was 3000 rpm.

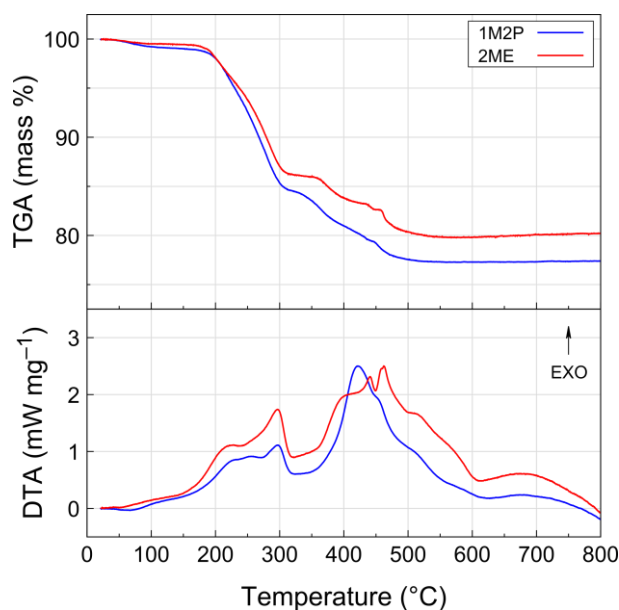


**Figure S8** – Thermal analysis of powders obtained by drying  $\text{PbTiO}_3$  solutions (90 °C, 12 h): thermogravimetric analysis (TGA) and differential thermal analysis (DTA). The elimination of residual organics in the powders likely occurs between 200 and 320 °C. From the DTA signal, it appears that the crystallization of 2ME-derived  $\text{PbTiO}_3$  occurs at higher temperatures than 1M2P-derived  $\text{PbTiO}_3$ , as indicated by the shift of the exothermic contributions between 400 and 500 °C. In addition, the 2ME-derived powder displays several exothermic contributions, probably due to the formation of intermediate phases. Measurements were carried out on an STA 409 PC thermal analyzer (Netzsch, Germany), with a heating rate of 10 °C  $\text{min}^{-1}$  under air atmosphere.

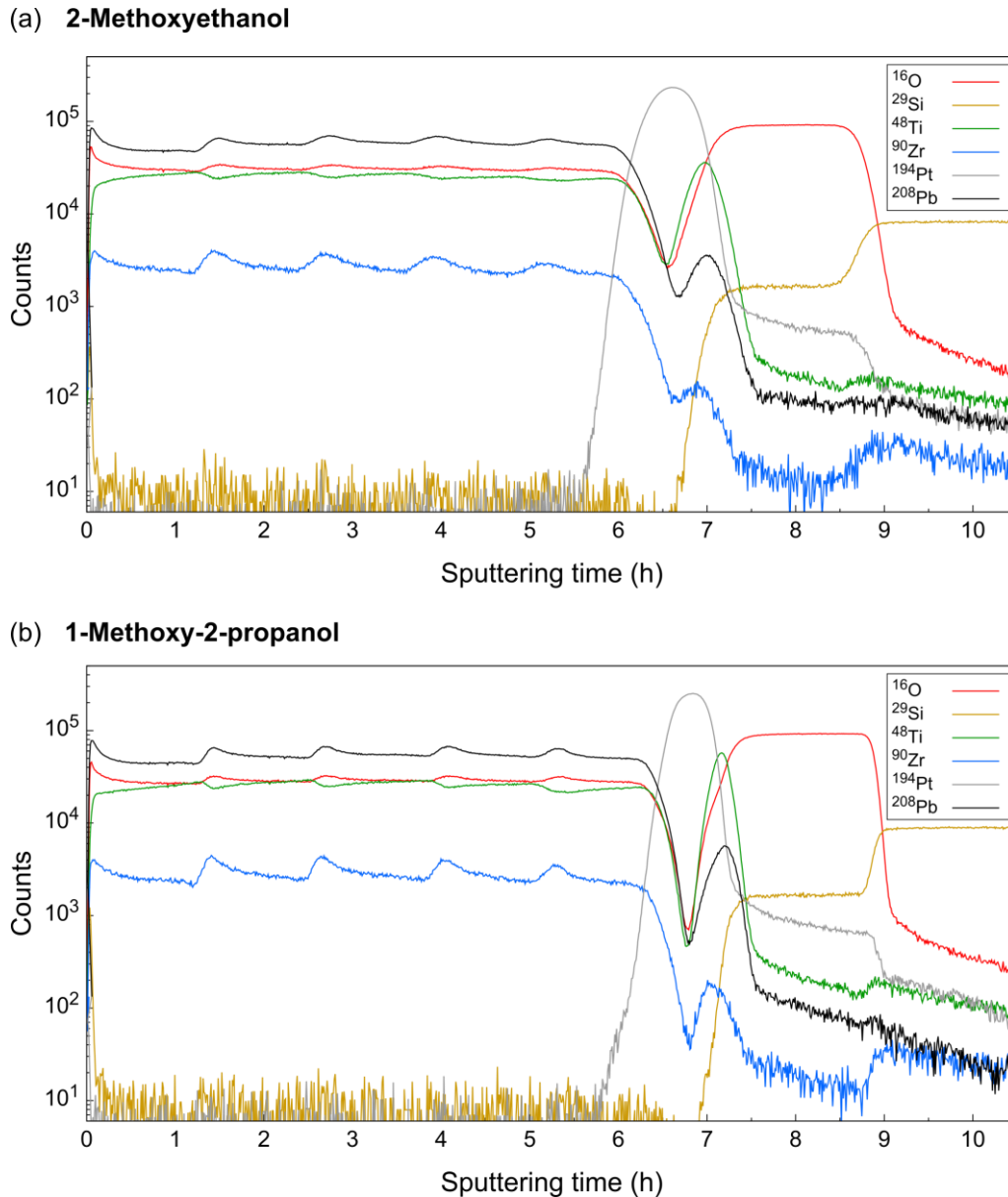


**Figure S9** – Dynamic secondary ion mass spectrometry (D-SIMS) depth profiling of (a) 2ME and (b) 1M2P-derived micron-thick PZT films. The primary ion beam ( $\text{Cs}^+$  ions) was accelerated at 1 keV and positive secondary ions were collected and analyzed in a 60  $\mu\text{m}$ -diameter spot. The five oscillations in the Zr and Ti signals are associated with the five deposition cycles (five crystallizations). Indeed, the crystallization of PZT proceeds through a Ti-rich phase, causing this characteristic sawtooth profile. In this experiment, the substrate was reached after  $\sim 6.5$  h of sputtering and its structure can be clearly identified (successively: Pt/TiO<sub>x</sub>/SiO<sub>2</sub>/Si).

A chemical gradient of Pb is also observed for each crystallized layer. Other studies already reported on PZT films exhibiting an increased Pb concentration at the surface (Y. Bastani and N. Bassiri-Gharb, *Acta Materialia*, 2012, **60**, 1346–1352; I. Gueye, G. Le Rhun, P. Gergaud, O. Renault, E. Defay and N. Barrett, *Applied Surface Science*, 2016, **363**, 21–28). This gradient could originate from the superstoichiometric amount of Pb (the solutions have 10% excess Pb) present in the as-deposited layers. As crystallization is initiated at the interface and proceeds upwards, forming the stoichiometric perovskite, Pb is segregated towards the surface. Sublimation of PbO also occurs, but does not completely suppress this effect.

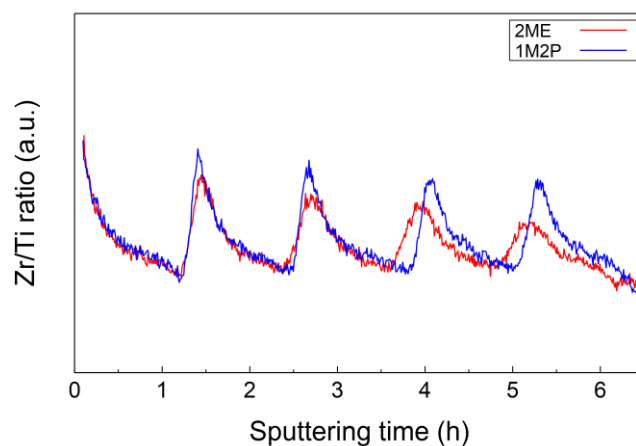


**Figure S10** – Evolution of the Zr/Ti ratio obtained from D-SIMS depth profiling of 2ME and 1M2P-derived PZT thin films. Ratios were calculated based on the absolute intensities (see Fig. S9). The gradient is quantitatively similar for both samples, but the 1M2P-derived PZT film exhibits a more pronounced gradient in the vicinity of the substrate, which can be correlated with the stronger {100} orientation induced in the layer due to higher extent of heterogeneous nucleation.